Long-range atomic order in $Ga_xIn_{1-x}As_yP_{1-y}$ epitaxial layers [$(x,y)=(0.47,1)$, $(0.37,0.82)$, $(0.34,0.71)$, and $(0.27,0.64)$]

M. A. Shahid and S. Mahajan
Department of Metallurgical Engineering and Materials Science, Carnegie-Mellon University, Pittsburgh, Pennsylvania 15213
(Received 9 November 1987)

Transmission-electron microscopy and selected-area diffraction have been used to study $Ga_xIn_{1-x}As_yP_{1-y}$ [$(x,y)=(0.47,1)$, $(0.37,0.82)$, $(0.34,0.71)$, and $(0.27,0.64)$] alloy semiconductors. A systematic analysis of edge-on and plane-view samples has shown that an ordered phase closely related to the CuPt-type structure exists in these materials. Only two of the possible four {111}-ordered variants are observed. An attempt is made to rationalize this observation and a detailed account of atomic ordering in these alloys (for a range of values of x and y) is presented.

I. INTRODUCTION

Pseudobinary III-V compound semiconductors are important materials because of their potential applications in modern optoelectronics and microwave devices such as laser diodes,[1] photodetectors,[2] and field-effect transistors.[3] Their band gap can be tailored by changing their composition in order to meet requirements for a specific application, e.g., laser diodes can be fabricated that emit at a particular wavelength where fused silica fibers used in current optical communication systems exhibit less attenuation. $Ga_{0.47}In_{0.53}As$ and $Ga_xIn_{1-x}As_yP_{1-y}$ [$(x,y)=(0.37,0.82)$, $(0.34,0.71)$, and $(0.27,0.64)$] are members of this family of III-V alloy semiconductors.

Epitaxial layers of these materials, lattice matched to InP substrates, can be grown using liquid-phase epitaxy (LPE),[4] metal-organic chemical-vapor deposition (MOCVD),[5] molecular-beam epitaxy (MBE),[6] and more recently vapor-levitation epitaxy (VLE).[7–10] Their thermodynamic,[11–16] materials,[17–23] optical,[24–26] and electronic[27–30] properties have been extensively studied. It has been noted that a miscibility gap exists in the phase diagram that leads to alloy clustering and/or phase separation.[12–20] This is observed to affect the mobility of carriers[31] and to produce broadening of a linewidth in a luminescence[32] spectrum of an optical device fabricated from these materials.

These alloy semiconductors crystallize in the zinc-blende (ZB) crystal structure ($F\bar{4}3m$).[33] This structure consists of two interpenetrating face-centered-cubic (fcc) sublattices of group-III and group-V atoms in which one sublattice is displaced with respect to the other by $a\sqrt{3}/4$ along the $\langle 111 \rangle$ direction, where a is the lattice constant. Furthermore, it is also believed that in a ternary and a quaternary III-V alloy semiconductor, both the group-III and group-V atoms, are randomly distributed in their respective sublattice(s) such that the resulting structure lacks long-range order. Contrary to this commonly held belief, extended x-ray-absorption fine-structure (EXAFS) measurements show that the nearest-neighbor (NN) distances deviate from their average value (following Vegard's law[34]) in $Ga_xIn_{1-x}As$ ($x=0-1$) and correspond to those of the Ga—As and In—As bond lengths in the unmixed binary constituent components, GaAs and InAs (Refs. 35 and 36), respectively. This indicates the existence of short-range order in this material due to atomic clustering. On the basis of next NN (NNN) and NN distance measurements, a chalcopyrite crystal structure for $Ga_{0.5}In_{0.5}As$ has been proposed.[35] The subsequent work, however, does not support this suggestion.[37–39]

Recently several authors have theoretically examined the possibility of long-range order in pseudobinary alloy semiconductors.[40–47] Taking $Ga_xIn_{1-x}As$ as a model system they have considered five possible arrangements in a unit tetrahedron; namely, Ga(4)In(0)As, Ga(3)In(1)As, Ga(2)In(2)As, Ga(1)In(3)As, and Ga(0)In(4)As (here numbers in the parentheses represent the number of respective atoms as NN's to an As atom located at the center of the unit tetrahedron in $Ga_{0.47}In_{0.53}As$). Using different models and approximations, these authors predict that at equilibrium there is a tendency for ordering rather than clustering. Similar conclusions have been derived for other ternary alloys. This is thought to be due to the ability of an ordered structure to accommodate two dissimilar bond lengths in a coherent fashion thereby reducing strain.

Within the last few years, several experimental reports of long-range order in different III-V ternary alloys,[37–39,43–46,48–54] $Ga_{0.37}In_{0.63}As_{0.82}P_{0.18}$,[38] $Ga_{0.51}In_{0.49}P$,[55] and SiGe (Ref. 56) have been published. These studies are important for two reasons. First, they provide guidance for modeling the structure of these alloys. Second, such ordered phases are expected to improve the transport properties of these materials significantly.[57,58] An interesting aspect of these studies is that they include materials which are completely miscible at the growth temperature, such as $Ga_xAl_{1-x}As$ (Refs. 48 and 51) ($x=0.15-0.80$) and those which show a miscibility gap in their phase diagram, for example, $GaAs_{0.5}Sb_{0.5}$,[49,53,54] $Ga_xIn_{1-x}As$ ($x=0.47$ or 0.5),[37–39] $Al_{0.5}In_{0.5}As$,[50] $Ga_{0.51}In_{0.49}P$,[52,55] and $Ga_{0.37}In_{0.63}As_{0.82}P_{0.18}$.[38] The reported structures of the ordered phases in III-V alloy semiconductors are the

following: Famatinite ($I\bar{4}2m$, Cu_3SbS_4-type) in $Ga_{0.47}In_{0.53}As$,[37] tetragonal ($P\bar{4}m2$, where one sublattice is ordered as CuAu I) in $Ga_xAl_{1-x}As$ ($x=0.15-0.80$),[48,51] $Ga_{0.5}In_{0.5}As$,[39] and $GaAs_{0.5}Sb_{0.5}$,[49,53,54] chalcopyrite ($I\bar{4}2d$, $CuFeS_4$-type) in $GaAs_{0.5}Sb_{0.5}$ (Ref. 49) and trigonal (CuPt-type) in Si/Ge strained layers,[56] $Ga_{0.47}In_{0.53}As$,[38] $Ga_{0.37}In_{0.63}As_{0.82}P_{0.18}$,[38] and $Al_{0.5}In_{0.5}As$.[50]

Since our brief report on the occurrence of an ordered phase in $Ga_{0.47}In_{0.53}As$ and $Ga_{0.37}In_{0.63}As_{0.82}P_{0.18}$,[38] closely related to the CuPt-type ordered structure,[59] we have investigated these materials in more detail and have also included the quaternaries $Ga_{0.34}In_{0.66}As_{0.71}P_{0.29}$ and $Ga_{0.27}In_{0.73}As_{0.64}P_{0.36}$ in our studies. We have used transmission-electron microscopy (TEM) and selected-area electron diffraction (SAD) to conduct a detailed analysis of the microstructure and symmetry of the ordered phases using both edge-on and plane-view samples. The observed ordered variants have been correlated with the crystallography of decomposition pits observed on the InP(001) surface. Our results indicate that only two of the possible four-ordered variants are present in these materials.

II. EXPERIMENTAL METHOD

Epitaxial layers of $Ga_{0.37}In_{0.63}As_{0.82}P_{0.18}$ (sample *A*), $Ga_{0.34}In_{0.66}As_{0.71}P_{0.29}$ (sample *B*), $Ga_{0.27}In_{0.73}As_{0.64}P_{0.36}$ (sample *C*), and $Ga_{0.47}In_{0.53}As$ (sample *D*), lattice matched to InP(001) substrates were grown by VLE; details of the growth process have been published elsewhere.[7–10] The structures of the layers in samples *A* and *D* have been detailed elsewhere,[38] whereas the samples *B* and *C* consisted of single quaternary layers on the InP substrates. The growth temperatures for the pairs of samples (*A* and *D*) and (*B* and *C*) were, respectively, 660 and 650 °C. While edge-on samples were prepared from all structures, the plane-view samples were prepared from *A*, *B*, and *C* samples only. For the edge-on samples, a pair of thin sections were cleaved along the [110] and [$\bar{1}$10] orthogonal directions. These sections were glued face to face along with a dummy sample (to be used as a reference). The final thinning of the edge-on samples was done using an Ar^+-ion milling machine at liquid-nitrogen temperature, whereas thinning for the plane-view samples was carried out in a solution of 1.5% bromine in methanol. In the case of double-heterojunction laser structure of sample *A*, the *n*-type InP surface layer was selectively etched off prior to chemical thinning. Finally, the samples were studied in a Philips EM420 electron microscope operating at 120 keV.

III. RESULTS

The plane-view samples *A*, *B*, and *C* did not show extra spots in the (001) SAD patterns. These samples were tilted in the microscope. A set of SAD patterns for the $(112)^*$, $(\bar{1}12)^*$, $(\bar{1}\,\bar{1}2)^*$, and $(1\bar{1}2)^*$ poles of the reciprocal lattice of sample *A* is shown in Figs. 1(a), 1(b), 1(c) and 1(d), respectively. A comparison of these SAD patterns shows that only two of the possible four {111} variants show extra spots. These extra reflections correspond to the (112) and ($\bar{1}\,\bar{1}2$) poles due to atomic ordering on ($\bar{1}\,\bar{1}1$) and (111) planes [Figs. 1(a) and 1(c)]. On the other hand, no superstructure spots are observed in the SAD patterns from the ($\bar{1}12$) and ($1\bar{1}2$) poles [Figs. 1(b) and 1(d)]. This is consistent with our results on the edge-on samples. While ($\bar{1}10$) edge-on samples show extra spots along the $\pm[\bar{1}\,\bar{1}1]$ and $\pm[111]$ directions halfway between the spots of the disordered matrix indicating atomic ordering on the ($\bar{1}\,\bar{1}1$) and (111) planes (Fig. 4 in Ref. 38), no extra spots are observed in the (110) edge-on samples. Similar experiments were carried out on samples *B*, *C*, and *D* and the results were identical to those of sample *A*. Although sample *D* showed extra spots at exactly similar positions (Fig. 2 in Ref. 38), the relative intensity of the spots was weak compared with the other three samples.

A set of TEM micrographs produced from the same area of the edge-on sample *A* using a set of different two beam conditions is shown in Fig. 2(a) ($\mathbf{g}\|[004]$) and 2(b) ($\mathbf{g}\|[\bar{2}\,\bar{2}0]$). While a strongly modulated structure, present on a coarse scale along the [110] projected direction, is clearly visible in Fig. 2(b), the (004) reflection reveals compositionally modulated structure along the growth direction [Fig. 2(a)] on a much finer scale. These micrographs also show that a major component of lattice strain in the epilayers lies in the growth plane. This sample was titled in the microscope through ±45° about [001] direction as an axis in order to investigate the contrast effects in the (100) and (010) planes. It was noted that the diffraction contrast due to spinodal decomposition or phase separation along the [100] and [010] directions are not equivalent. It was also found that the elastic lattice strain due to spinodal decomposition or phase separation, on a coarse scale, was predominently along the [100] direction; although relatively weak modulated structure of a similar character was also present along the [010] direction. This was in addition to the fine-scale quasi-periodic structure which was present in all the three cube directions. Moreover, the SAD patterns for the (001) and (010) poles were similar to that of the (001) pole and showed no extra spots. Using the (004) spots in these SAD patterns as a calibration, an attempt was made to measure the tetragonal distortion along the [100] and [010] cube directions. No difference in the lattice constant along these directions could be measured.

Lastly, planar samples, one each from *A* and *D*, were annealed in a flowing forming gas (a mixture of 10% H_2 in N_2) atmosphere at 650 °C for 15 min without surface protection. This results in thermal decomposition of InP due to preferential loss of more volatile P and hence produces rectangular thermal decomposition pits on an InP(001) sample.[60,61] A comparison of the shape of these pits and the ordered variants seen in the edge-on samples shows that the observed ordered variants correspond to the $(\bar{1}\,\bar{1}\,1)_{In}$ and $(111)_{In}$ facets of the decomposition pit.

IV. DISCUSSION

In order to describe the properties of III-V ternary and quaternary alloy semiconductors, the virtual crystal approximation has often been used.[62] In this approximation

all the constituent atoms are located in their respective sublattices at ideal lattice points defined by an average lattice constant (following Vegard's law[34]). Moreover, the local distortions are ignored and all the atoms are assumed to carry average values of bond length, ionicity, potential, etc. Obviously such a model cannot justify the presence of the superlattice spots in Figs. 1(a) and 1(c). On the other hand, Mikkelson and Boyce[35,36] have used EXAFS studies to show that the NN distances in $Ga_xIn_{1-x}As$ ($x=0-1$) are very close to the In—As and Ga—As bond lengths in the unmixed InAs and GaAs binary compounds, respectively. They have also shown that a distribution of unequal (by about 7%) bonds in $Ga_xIn_{1-x}As$ is present. Therefore, the total energy of the system includes a significantly large strain term. This arises from the fact that two (and more in the quaternary systems) unequal bond lengths set up bond-stretching and bond-bending forces. The nature of these forces will depend on the arrangements of atoms in the basic tetrahedral unit cell (and, of course, distribution of these unit cells).

Before going into the details of the arrangement of atoms in the unit cells, let us briefly introduce the most obvious crystal structures of the III-V ternary alloys closely related to and derived from the zinc-blende structures. In these crystal structures, one of the two fcc sub-

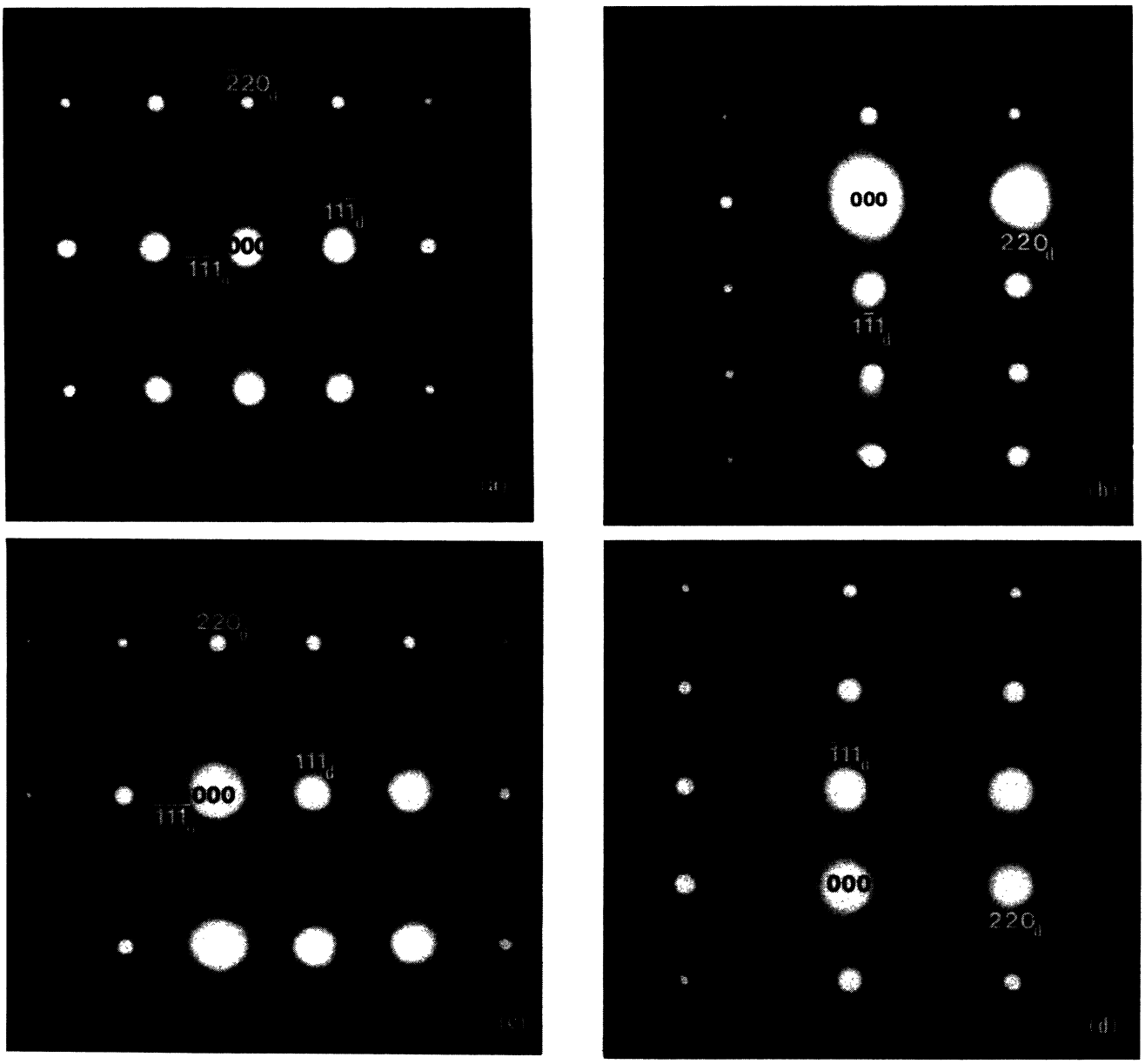

FIG. 1. A set of SAD patterns showing the (a) $(112)^*$, (b) $(\bar{1}12)^*$, (c) $(\bar{1}\,\bar{1}2)^*$, and (d) $(1\bar{1}2)^*$ poles of the reciprocal lattice of sample *A*. Notice extra spots are present halfway between the matrix spots along the $\langle 111 \rangle$ directions in (a) and (c) only. The indices with subscripts *d* and *o* represent reflections from disordered and ordered phases, respectively.

lattices consists of the atoms of the same group (group III or group V depending on whether the ternary is $A^{III}B_x^VC_{1-x}^V$ or $A_x^{III}B_{1-x}^{III}C^V$). On the second fcc sublattice, the lattice positions are occupied by a mixture of atoms (from group III or group V) such that the resulting structure can be defined by one of the following crystal structures: (a) chalcopyrite ($CuFeS_2$-type, $I\bar{4}2d$), (b) simple tetragonal (CuAu I, $P\bar{4}m2$), (c) luzonite (Cu_3AsS_4-type, $P\bar{4}3m$), and (d) famatinite (Cu_3SbS_4-type, $I\bar{4}2m$).[46]

Figure 3 shows a set of three schematic arrangements of the tetrahedral unit cells, namely, Ga(1)In(3)As, Ga(2)In(2)As, and Ga(3)In(1)As for the three values of the composition parameter $x=0.25$, 0.5, and 0.75, respectively, in $Ga_xIn_{1-x}As$ (note that $x=0.5$ can also be obtained by an equal mixing of $x=0.25$ and $x=0.75$ as will be discussed later). It is readily evident that in the case of Ga(2)In(2)As, because of $\sim 7\%$ difference in the In—As and Ga—As bond lengths, the equilibrium position of the central As atom will be displaced along that $\langle 100 \rangle$ cube direction which joins the midpoints of the Ga-Ga and In-In atom positions thereby distorting the tetrahedral unit cell. On the other hand, in both Ga(3)In(1)As and Ga(1)In(3)As configurations, displacement of the As atom will be along that $\langle 111 \rangle$ direction which lies along the In(1)—As or Ga(1)—As bonds, respectively. Clearly the tetrahedral unit cell suffers from distortion in this case also but it is different from the former. Therefore, the nature and extent of lattice strain in the crystal will depend both on the arrangement and distribution of these tetrahedral building blocks in the resulting structure.

The results of the present experiment indicate that none of the SAD patterns from $Ga_{0.47}In_{0.53}As$ and

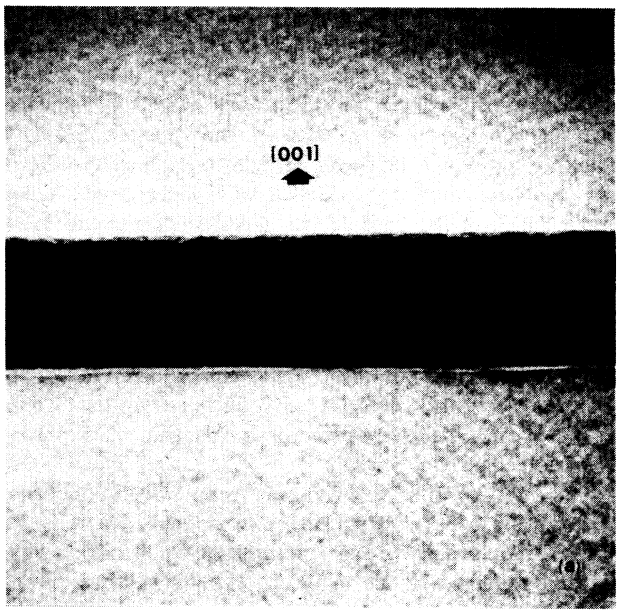

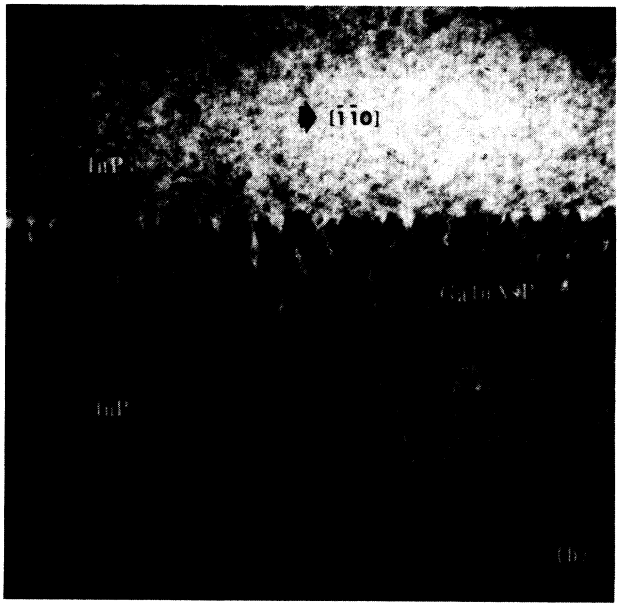

FIG. 2. A set of bright field TEM micrographs produced from sample A (edge-on views) using two beam conditions: (a) $\mathbf{g}\|[004]$ and (b) $\mathbf{g}\|[\bar{2}\bar{2}0]$. The $\mathbf{g}$ vectors have been indicated by the arrows. Notice the differences in contrast in these images. Width of the quaternary layer is 0.25 μm.

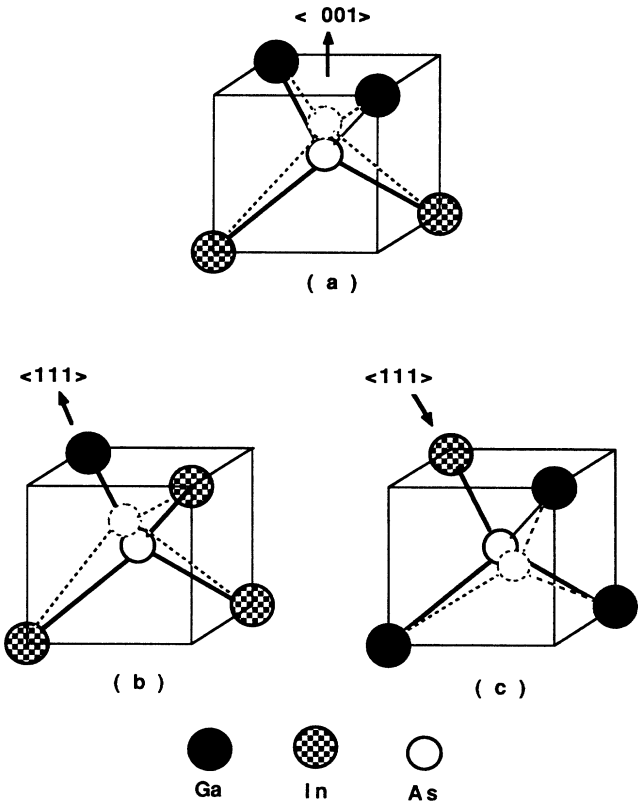

FIG. 3. A set of schematic drawings showing the atomic arrangements in ordered $Ga_xIn_{1-x}As$ tetrahedral unit cell. (a) Ga(2)In(2)As for $x=0.5$, (b) Ga(3)In(1)As for $x=0.75$, and (c) Ga(1)In(3)As for $x=0.25$. While in an unmixed GaAs or InAs, the As atom is located at the body center of the tetrahedral unit cell, in the mixed unit cells, the As atoms shifts to a new position (shown by a dotted circle) thereby distorting the unit cell (see text for details). Notice the $Ga_xIn_{1-x}As$ alloy for $x=0.5$ can also be obtained by stacking (b) and (c) alternately along the In(1)As [111] direction.

$Ga_xIn_{1-x}As_yP_{1-y}$ [$(x,y)=(0.37,0.82)$, (0.34,0.71), and (0.27,0.64)] [except for the (001) pole] matches those resulting from the crystal structures described above.[46] Although the famatinite structure for $Ga_{0.47}In_{0.53}As$ has been reported,[37] it is not clear whether it is due to Ga(3)In(1)As or Ga(1)In(3)As (or both). These two tetrahedral descriptions correspond to $x=0.75$ and $x=0.25$, respectively, and either of these two structures could produce the superstructure reported by Nakayama and Fujita.[37] However, this implies a large compositional change (by $\sim 100\%$) from a nominal value of $x=0.47$ used to grow this material lattice matched to InP. Moreover, the sizes of the ordered domains reported by Nakayama and Fujita are relatively large which is difficult to justify in the light of extremely small diffusion coefficients for both In and Ga atoms at the growth temperature of their experiment (~ 650 °C).

The SAD patterns of the present experiment match those expected from a CuPt-type trigonal ($R\bar{3}m$ symmetry) ordered phase.[59] Although Ga(3)In(1)As and Ga(1)In(3)As configurations similar to those in the famatinite structure of Nakayama and Fujita[37] are also involved in the trigonal structure, the arrangements of these configurations is distinctly different in these two structures. While in the famatinite structure either Ga(3)In(1)As *or* Ga(1)In(3)As ($x=0.75$ *or* $x=0.25$) is required to produce the desired results, in the trigonal structure *both* Ga(3)In(1)As *and* Ga(1)In(3)As ($x=0.5$) are stacked alternately on top of each other along the ordered $\langle 111 \rangle$ direction. This doubles the real-space translation period along this direction. Moreover, due to lack of a center of symmetry in the ZB lattice, the observed structure belongs to the $R3m$ system. A computer generated SAD pattern from such a structure shows excellent agreement with the SAD pattern of our experiment (Fig. 3 in Ref. 38). Moreover, we have not compared the strain energies associated with the famatinite and trigonal structures and similar results are also not available for these systems. However, on the basis of our experimental data it appears that the trigonal phase represents a relatively lower energy state since it accommodates two dissimilar bond lengths in a coherent manner.

It must be pointed out that there are important differences in the bonding arrangement of the conventional CuPt-type (in which SiGe alloy orders[56]) and the one observed in $Ga_{0.47}In_{0.53}As$ and $Ga_xIn_{1-x}As_yP_{1-y}$ alloys [$(x,y)=(0.37,0.82)$, (0.34,0.71), and (0.27,0.64)]. A set of projections of the $\{111\}$ planes in the real space is schematically shown in Fig. 4 for these structures to highlight these differences. The interplanar spacings for all the systems have been shown equal to each other for clarity. In this figure the solid lines represent the positions of the atomic planes. A comparison of these drawings clearly demonstrates the origin of the superlattice reflections at the $\frac{1}{2}\langle 111 \rangle$ and equivalent positions (of the disordered matrix) in the SAD patterns in the ordered SiGe,[56] $Ga_{0.5}In_{0.5}As$,[38] and $Ga_{0.5}In_{0.5}As_{0.5}P_{0.5}$ (Ref. 38) (and also other similarly ordered structures such as $Al_{0.5}In_{0.5}As$, $GaAs_{0.5}Sb_{0.5}$, and $Ga_{0.5}In_{0.5}P$) alloys because in the ordered phase the real-space period is twice

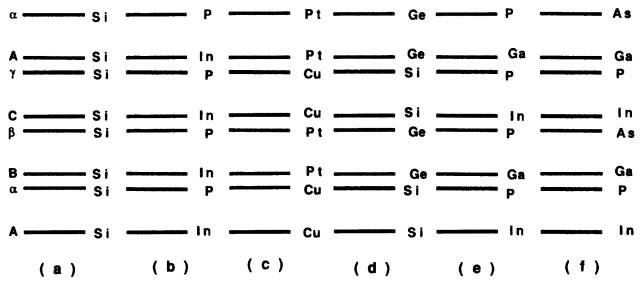

FIG. 4. Schematic drawings showing the traces of (111) planes in (a) Si, (b) InP, (c) ordered CuPt, (d) ordered SiGe, (e) ordered $Ga_{0.5}In_{0.5}As$, and (f) ordered $Ga_{0.5}In_{0.5}As_{0.5}P_{0.5}$. Notice the differences in the ways the real-space period doubles in the ordered CuPt and ordered $Ga_{0.5}In_{0.5}As$ and $Ga_{0.5}In_{0.5}As_{0.5}P_{0.5}$.

that of the disordered phase in the ordered $\langle 111 \rangle$ direction. It is also evident that in the ordered SiGe, the stacking sequence consists of Si-Si(αA) and Ge-Ge(βB) $\{111\}$ planes along the ordered $\langle 111 \rangle$ direction. On the other hand, in the case of $Ga_{0.5}In_{0.5}As$ ternary alloy, the stacking sequence in the ordered $\langle 111 \rangle$ direction is $\cdots AsIn_rAsGa_rAsIn_rAs \cdots$ and in the case of the quaternary $Ga_{0.5}In_{0.5}As_{0.5}P_{0.5}$ alloy it is $\cdots As_rIn_rP_rGa_rAs_rIn_rP_rGa_rAs_r \cdots$. Here the subscript r indicates that, for instance, for $Ga_r(111)$ plane, the Ga-to-In ratio is significantly larger than that defined by the composition parameter x (so that this plane is "Ga-rich" and vice versa).

The question that still remains unanswered concerns as to how this ordered structure is formed. In a recent report, Kuan *et al.*[39] have shown that an ordered phase, closely related to the CuAuI-type structure, is also present in an epitaxial layer of $Ga_{0.5}In_{0.5}As$. However, the conditions of their experiment are different from ours. For instance, they have used a InP(110) substrate to grow their epilayers by MBE. This indicates that the structure of an ordered phase is strongly dependent on the orientation of the substrate.

The presence of two ordered variants in our experiments instead of four may be rationalized in terms of faceted growth. Prior to the initiation of epitaxial growth, an InP substrate is heated in the growth chamber to bring it to the desired temperature. This has the effect of producing facets on the substrate surface due to thermal decomposition, degree of which depends on the type of the substrate, temperature, and the time for which the substrate gets heated. Under such conditions, relatively longer $\{111\}_{In}$ facets are exposed due to prefernetial loss of P (Refs. 60 and 61) [a similar argument can be invoked to justify the observed ordered structure in $Al_{0.5}In_{0.5}As$, $Ga_{0.51}In_{0.49}P$, and $GaAs_{0.5}Sb_{0.5}$ epitaxial layers grown on the GaAs(001) substrates]. We believe that this initial bias in the substrate surface is responsible for the occurrence of the only two ordered variants. Furthermore, a study of relative intensities of the ordered variants in the SAD patterns indicates that one variant is stronger than the other. This could be related to the surface misorientation which may bias one of the two variants.

As discussed earlier, these alloys are known to have a miscibility gap in their phase diagrams. In a recent more refined investigation, Czyzyk *et al.*[42] have shown the existence of this miscibility gap at certain values of the composition parameter. This results in the development of the well-known concentration waves in the ⟨100⟩ soft directions of these alloys. In a TEM micrograph, these appear as a "basket-weave" pattern of black-white contrast while in the corresponding SAD pattern a set of satellite reflections may appear along the directions of composition modulation.[20] The results of Fig. 2 clearly show the evidence of spinodal decomposition or phase separation in these materials. However, the present experiment also shows that in the epilayers the three cube directions are not equivalent to each other. The concentration waves showing a quasiperiodic structure at a relatively long period are observed predominently along the [100] and [010] directions, the former being relatively stronger of the two. On the other hand, the [001] growth direction only shows a fine-scale quasiperiodic structure which is also seen along the other two cube directions (in a well-developed spinodal it is this fine-scale periodic structure which produces observable satellite diffraction spots in an SAD pattern). At present it is not clear what is the source of this anisotropic behavior. It could be related to an asymmetric strain which may result from the observed ordered variants of a significantly different degree.

When ordering and phase separation occur in an alloy system, the following three distinct situations could arise: (i) ordering precedes phase separation (ii) phase separation precedes ordering, and (iii) the two occur concomitantly. Since the computed critical temperatures for phase separation in these alloy semiconductors are considerably lower than the observed ones,[16,17] it has been argued that phase separation occurs at surface regions during growth.[19(b)] Ordering may also take place in the surface regions because type of the ordered structure is affected by the substrate orientation.[39] It is therefore conceivable that ordering and phase separation occur concomitantly, as envisaged in the metallic systems.[63,64]

The results presented in this paper are important because they enhance our understanding of the structure of pseudobinary III-V compound semiconductors in general and $Ga_{0.47}In_{0.53}As$ and $Ga_xIn_{1-x}As_yP_{1-y}$ $[(x,y)=(0.37,0.82), (0.34,0.71)$, and $(0.27,0.64)]$ in particular. The ordered phase which we have discovered in these materials represents a modulated structure in the ⟨111⟩ direction and may provide a natural source of carrier confinement on an atomic scale. In such an ordered phase the mobility of the carriers is expected to be extremely high since the interplanar spacing, $d_{\langle 111\rangle}$, is the largest in these structures providing relatively wide channels for the transport of the carriers. Lastly, if the source of atomic ordering is related with the charge transfer between the participating atomic species,[27,65] then this ordered structure represents a coherently layered structure and defines a system of charge-density waves on an atomic scale in the ⟨111⟩ ordered directions which in itself should show interesting properties.

V. SUMMARY

A systematic analysis on the $Ga_xIn_{1-x}As_yP_{1-y}$ $[(x,y)=(0.47,1), (0.37,0.82), (0.34,0.71)$, and $(0.27,0.64)]$ epitaxial layers have shown that atomic ordering occurs on {111} planes. Only two of the possible four ordered variants are observed and these variants correspond to the $(\bar{1}\,\bar{1}1)_{In}$ and $(111)_{In}$ facets of a thermally induced decomposition pit on the InP(001) surface. While only fine-scale quasiperiodic structure due to spinodal decomposition develops along the [001] growth direction, both coarse and fine quasiperiodic modulations are observed along the [100] and [010] directions. It is suggested that ordering and phase separation occur concomitantly in these alloy semiconductors.

ACKNOWLEDGMENTS

The authors would like to thank Dr. H. M. Cox for supplying the samples studied during this work and Professor D. E. Laughlin for fruitful discussions. The authors also wish to acknowledge the financial support of the National Science Foundation through Grant No. DMR-8405624 and the U.S. Department of Energy through Grant No. DE-FG02-87ER45329.

[1]H. Ohno and J. Barnard, in *GaInAsP Alloy Semiconductors,* edited by T. P. Pearsall (Wiley, New York, 1982), Chap. 17, p. 437.

[2]Y. Suematsu, K. Iga, and K. Kishino, in *GaInAsP Alloy Semiconductors,* Ref. 1, Chap. 14, p. 341.

[3]Y. Matsushima and K. Sakai, in *GaInAsP Alloy Semiconductors,* Ref. 1, Chap. 16, p. 413.

[4]K. Nakajima, in *GaInAsP Alloy Semiconductors,* Ref. 1, Chap. 2, p. 43.

[5]J. P. Hirtz, M. Razeghi, M. Bonnet, and J. P. Duchemin, in *GaInAsP Alloy Semiconductors,* Ref. 1, Chap. 3, p. 61.

[6]C. E. Wood, in *GaInAsP Alloy Semiconductors,* Ref. 1, Chap. 4, p. 87.

[7]H. M. Cox, J. Cryst. Growth **69**, 641 (1984).

[8]H. M. Cox, M. A. Koza, and V. G. Keramidas, J. Cryst. Growth **73**, 523 (1985).

[9]H. M. Cox, S. G. Hummel, and V. G. Keramidas, J. Cryst. Growth **79**, 900 (1986).

[10]H. M. Cox, S. G. Hummel, V. G. Keramidas, and H. Temkin, in *Institute of Physics Conference Proceedings Series* (IOP, Bristol, 1986), Vol. 79, p. 735.

[11]M. S. Abrahams, R. Braunstein, and F. D. Rosi, J. Phys. Chem. Solids **10**, 204 (1959).

[12]B. DeCremoux, IEEE J. Quantum Electron. **QE-2**, 123 (1981).

[13]G. B. Stringfellow, J. Cryst. Growth **27**, 21 (1974).

[14]J. J. Hsieh, IEEE J. Quantum Electron. **QE-17**, 118 (1981).

[15]K. Onabe, Jpn. J. Appl. Phys. **21**, L323 (1982).

[16]G. B. Stringfellow, J. Cryst. Growth **58**, 194 (1982).

[17]P. Henoc, A. Izrael, M. Quillec, and H. Launois, Appl. Phys. Lett. **40**, 963 (1982).

[18]S. Mahajan, B. V. Dutt, H. Temkin, R. J. Cava, and W. A. Bonner, J. Cryst. Growth **68**, 589 (1984).
[19](a) S. N. G. Chu, A. T. Macrander, K. E. Sterge, and W. D. Johnston, Jr., J. Appl. Phys. **57**, 249 (1985); (b) S. N. G. Chu, S. Nakahara, K. E. Sterge, and W. D. Johnston, Jr., *ibid.* **57**, 4610 (1985).
[20]A. G. Norman and G. R. Booker, J. Appl. Phys. **57**, 4715 (1985).
[21]O. Ueda, S. Isozumi, and S. Komiya, Jpn. J. Appl. Phys. **23**, L241 (1984).
[22]G. P. Kuo, S. K. Vong, R. M. Cohen, and G. B. Stringfellow, J. Appl. Phys. **57**, 5428 (1985).
[23]T. Inoshita, J. Appl. Phys. **56**, 2056 (1984).
[24]C. Pickering, J. Electron. Mater. **10**, 901 (1981).
[25]See, for example, *Semiconductors and Semimetals,* edited by W. T. Tsang (Academic, New York, 1985), Vol. 22, Pts. B and C.
[26]T. P. Pearsal and T. P. Hirtz, J. Cryst. Growth **54**, 127 (1981).
[27]W. I. Wang, Solid State Electron. **29**, 133 (1986).
[28]E. O. Gobel, in *GaInAsP Alloy Semiconductors,* Ref. 1, Chap. 13, p. 313.
[29]J. D. Oliver, Jr., L. F. Eastman, P. D. Kirchner, and J. F. Schaff, J. Cryst. Growth **54**, 64 (1985).
[30]J. L. Pelloie, G. Guillot, A. Nouaihat, and A. G. Antolini, J. Appl. Phys. **59**, 1536 (1985).
[31]See, for example, Y. Takeda, in *GaInAsP Alloy Semiconductors,* Ref. 1, Chap. 9, and references therein.
[32]C. Charreaux, G. Guillot, and A. Nouaihat, J. Appl. Phys. **60**, 768 (1986).
[33]J. C. Philips, *Bonds and Bands in Semiconductors* (Academic, New York, 1973), pp. 11–14.
[34]L. Vegard, Z. Phys. **5**, 17 (1921).
[35]J. C. Mikkelson, Jr. and J. B. Boyce, Phys. Rev. B **28**, 7130 (1983).
[36]J. C. Mikkelson, Jr. and J. B. Boyce, Phys. Rev. Lett. **49**, 1412 (1982).
[37]H. Nakayama and H. Fujita, in *Institute of Physics Conference Proceedings Series,* Ref. 10, Vol. 79, p. 287.
[38]M. A. Shahid, S. Mahajan, D. E. Laughlin, and H. M. Cox, Phys. Rev. Lett. **58**, 2567 (1987).
[39]T. S. Kuan, W. I. Wang, and E. L. Wilkie, App. Phys. Lett. **51**, 51 (1987).
[40]F. Fukui, J. Appl. Phys. **57**, 5188 (1985).
[41]M. Ichimura and A. Sasaki, J. Appl. Phys. **60**, 3850 (1986).
[42]M. T. Czyzyk, M. Podgo'rny, A. Balzarotti, P. Letardi, N. Motta, A. Kisiel, and M. Zimanl-Starnawska, Z. Phys. B **62**, 153 (1986).
[43]A. Balzarotti, P. Letardi, and N. Motta, Solid State Commun. **56**, 471 (1985).
[44]G. P. Srivastava, J. L. Martins, and A. Zunger, Phys. Rev. B **31**, 2561 (1985).
[45]A. Zunger, Appl. Phys. Lett. **50**, 164 (1987).
[46]J. L. Martins and A. Zunger, J. Mater. Res. **1**, 523 (1986).
[47]A. A. Mbay, L. G. Ferreira, and A. Zunger, Phys. Rev. Lett. **58**, 49 (1987).
[48]T. S. Kuan, T. F. Kuech, W. I. Wang, and E. L. Wilkie, Phys. Rev. Lett. **54**, 201 (1985).
[49]H. R. Jen, M. J. Cherng, and G. B. Stringfellow, Appl. Phys. Lett. **48**, 1603 (1986).
[50]A. G. Norman, R. E. Mallard, I. J. Murgatroyd, G. R. Booker, A. H. Moore, and M. D. Scott, in *Institute of Physics Conference Proceedings Series* (IOP, Bristol, 1987), Vol. 87, p. 77.
[51]T. S. Kuan, in *Proceedings of the Forty-fourth Annual Meeting of The Electron Microscopy Society of America, Albuquerque, New Mexico, 1986,* edited by G. W. Baily (San Francisco Press, San Francisco, 1986), p. 398.
[52]A. Gomyo, T. Suzuki, K. Kobayashi, S. Kawata, and I. Hino, Appl. Phys. Lett. **50**, 673 (1987).
[53]Y. Ihm, N. Otsuka, J. Klem, and H. Morkoc, Appl. Phys. Lett. **51**, 2013 (1987).
[54]I. J. Murgatroyd, A. G. Norman, G. R. Booker, and T. M. Kerr, *Proceedings of the 11th International Congress on Electron Microscopy, Kyoto, 1986,* edited by T. Imura, S. Maruse, and T. Suzuki, (Japanese Society of Electron Microscopy, Tokyo, 1986), p. 1497.
[55]O. Ueda, M. Takikawa, J. Komeno, and I. Umebu, Jpn. J. Appl. Phys. **26**, L1824 (1987).
[56]A. Ourmazd and J. C. Bean, Phys. Rev. Lett. **55**, 765 (1985).
[57]A. E. Asch and G. L. Hall, Phys. Rev. **132**, 1047 (1963).
[58]J. Singh, IEEE Electron. Dev. Lett. **EDL-7**, 436 (1986).
[59]J. P. Chevalier and W. M. Stobbs, Acta. Metall. **27**, 285 (1979).
[60]W. Y. Lum and A. R. Clawson, J. Appl. Phys. **50**, 5296 (1979).
[61]S. Mahajan and A. K. Chin, J. Cryst. Growth **54**, 138 (1981).
[62]See Ref. 33, p. 212.
[63]D. E. Laughlin, K. B. Alexander, and L. L. Lee, in *Decomposition of Alloys: The Early Stages,* edited by P. Hassen, V. Gerold, R. Wagner, and M. F. Ashby (Pergamon, New York, 1984), p. 221.
[64]W. A. Soffa and D. E. Laughlin, in *Solid Phase Transformations,* edited by H. I. Aaronson, D. E. Laughlin, R. F. Sekerka, and C. M. Wayman (The Metallurgical Society of the AIME, Warrendale, PA, 1982), p. 159.
[65]W. I. Wang, J. Appl. Phys. **58**, 3244 (1985).

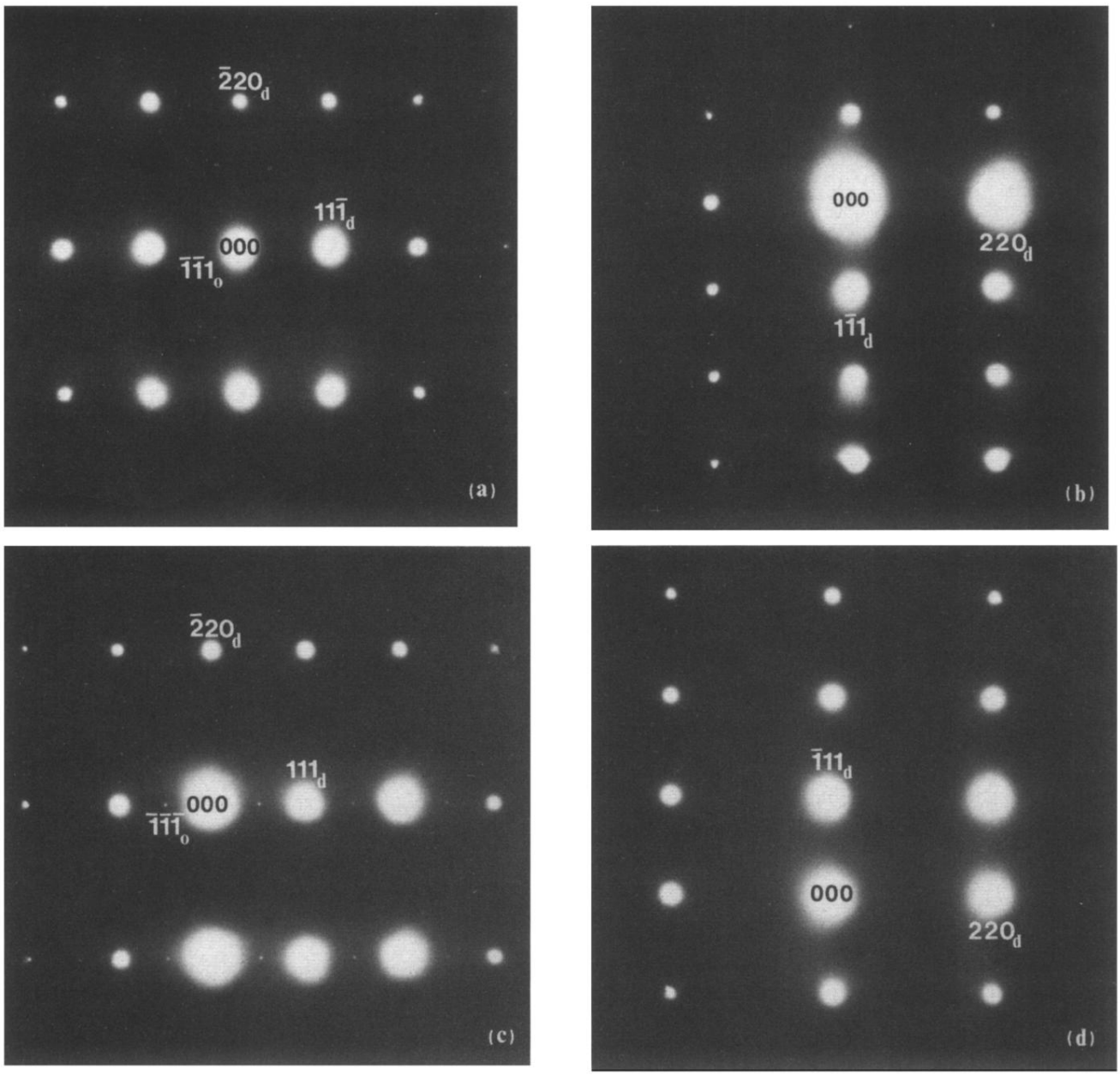

FIG. 1. A set of SAD patterns showing the (a) $(112)^*$, (b) $(\bar{1}12)^*$, (c) $(\bar{1}\,\bar{1}2)^*$, and (d) $(1\bar{1}2)^*$ poles of the reciprocal lattice of sample *A*. Notice extra spots are present halfway between the matrix spots along the $\langle 111 \rangle$ directions in (a) and (c) only. The indices with subscripts *d* and *o* represent reflections from disordered and ordered phases, respectively.

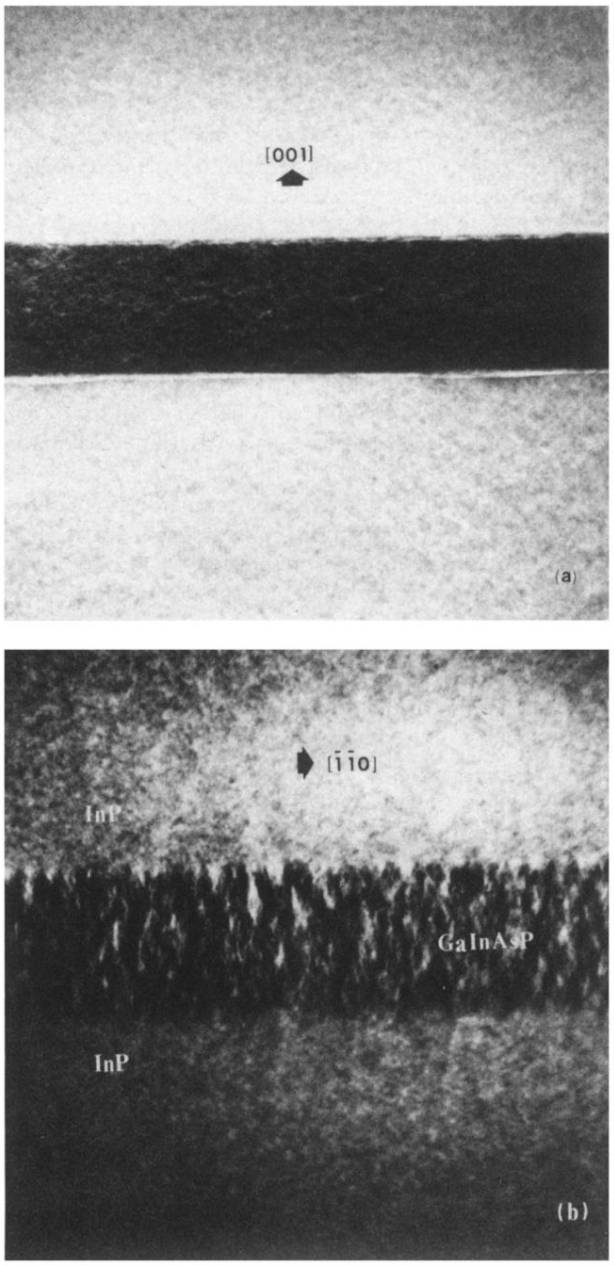

FIG. 2. A set of bright field TEM micrographs produced from sample *A* (edge-on views) using two beam conditions: (a) $\mathbf{g}\|[004]$ and (b) $\mathbf{g}\|[\bar{2}\,\bar{2}0]$. The **g** vectors have been indicated by the arrows. Notice the differences in contrast in these images. Width of the quaternary layer is 0.25 μm.